Nuclear Materials and Energy 34 (2023) 101363

Contents lists available at ScienceDirect

Nuclear Materials and Energy

journal homepage: www.elsevier.com/locate/nme

First feedback-controlled divertor detachment in W7-X: Experience from TDU operation and prospects for operation with actively cooled divertor

M. Krychowiak [a,*], R. König [a], T. Barbui [b], S. Brezinsek [c], J. Brunner [a], F. Effenberg [b], M. Endler [a], Y. Feng [a], E. Flom [d,a], Y. Gao [a], D. Gradic [a], P. Hacker [a], J.H. Harris [e], M. Hirsch [a], U. Höfel [a], M. Jakubowski [a], P. Kornejew [a], M. Otte [a], A. Pandey [a], T.S. Pedersen [a], A. Puig [a], F. Reimold [a], O. Schmitz [d], T. Schröder [a], V. Winters [a], D. Zhang [a], W7-X team [1]

[a] Max Planck Institute for Plasma Physics, 17491 Greifswald, Germany
[b] Princeton Plasma Physics Laboratory, Princeton, NJ 08543, USA
[c] Institute of Energy- and Climate Research, Forschungszentrum Jülich GmbH, D-52425 Jülich, Germany
[d] University of Wisconsin, Department of Engineering Physics, 1500 Engineering Drive, Madison, WI 53706, USA
[e] Oak Ridge National Laboratory, Oak Ridge, TN 37831, USA

ARTICLE INFO

MSC:
00-01
99-00

Keywords:
Plasma control
Detachment
Plasma fuelling and seeding

ABSTRACT

In the last experimental campaign (OP1.2b) of the stellarator Wendelstein 7-X (W7-X), boronisation as a mean for first wall conditioning was applied for the first time which led to strongly reduced impurity fluxes from plasma-facing components. Thermal detachment at the uncooled target plates of the test divertor unit (TDU) was reached at higher plasma densities and was accompanied by high recycling of neutrals at the target plate [1], [2]. A feedback control system was established in W7-X to actively control the gas injection (actuator) for plasma fuelling and impurity seeding [3] through the divertors. It allowed very successful stabilisation of the detached plasma condition state as well as mitigation of thermal overloads to some baffle tiles. Different routinely available diagnostic signals were used as input parameters (sensors). We describe the setup of the feedback control system, its performance and provide some example results with the main focus on the development of the control scheme which led to the detachment stabilisation over the entire longest (30 s) high-power discharge at W7-X so far. In view of the achieved very successful detachment stabilisation and the necessity to include simultaneous optimisation of the core performance in the future, the feedback control system is being upgraded for the upcoming campaign (OP2.1) in which the water cooled and hereby inherently steady-state capable divertor has been currently installed. The prospects and some experiment ideas for active detachment control are discussed.

1. Introduction

Wendelstein 7-X is the largest advanced superconducting stellarator, built to demonstrate quasi steady-state operation with strongly reduced neoclassical and fast particle losses. It started its first operation with uncooled limiters 2015 and was equipped for the two next campaigns (OP1.2a and OP1.2b) with ten uncooled graphite test divertor units. The boronisation applied for the first time during the OP1.2b campaign as a mean of first wall conditioning opened a path to high density operation accessing line-of-sight integrated electron densities up to $1.6{\times}10^{20}$ m^{-2}. At these high densities, thermal detachment of the plasma from all divertor plates was achieved meaning a strong reduction of the peak heat loads to the divertors by factor 10 (see Fig. 9 middle panel). It was accompanied by high recycling of neutrals at the target plate [1], [2]. Neutral pressures of up to 8×10^{-3} mbar were reached in the divertor providing particle pumping rates balancing the total amount of fuelled hydrogen. These two prerequisites allowed significantly longer stable detached discharges of up to 30 s limited only by heating up of the uncooled first wall components. Stabilisation of such long discharges can be realised by feedback control of the main plasma actuators. In our case a simple scheme turned out to provide a very robust detachment stabilisation: we controlled the fuelling or seeding gas flow rates of the fast divertor gas injection system while keeping the plasma electron cyclotron resonance heating (ECRH) power at a constant maximum available level of approx. 6 MW. The total plasma

* Corresponding author.
E-mail address: cak@ipp.mpg.de (M. Krychowiak).
[1] Thomas Sunn Pedersen et al. 2022 Nucl. Fusion 62 042022.

https://doi.org/10.1016/j.nme.2023.101363
Received 30 June 2022; Received in revised form 14 December 2022; Accepted 4 January 2023
Available online 10 January 2023

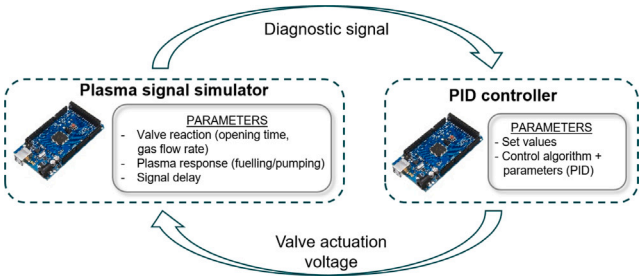

Fig. 1. Test electronic setup for tuning of the PID parameters.

radiation P_{rad} showed typically monotonic dependence on the line-integrated electron density in a transition into detachment [4]. This made the electron density a very good proxy for the level of detachment and provided a very robust way of detachment stabilisation which was also achieved using the carbon line emission in the divertor. Direct control of P_{rad} was also used but led to oscillations due to delayed signal reaction at the controller (see Sections 2, 3 and 4). Simple proportional/integral/derivative (PID) control algorithm was applied without the necessity to consider more complex physics models (recent applications of different types of control schemes in fusion plasmas can be found e.g. in [5–8]). The control parameters were pre-optimised using an electronic hardware simulator of the plasma diagnostic signals in a lab test setup which provided very good starting points for real W7-X discharges (see Fig. 1). We describe in Section 2 the newly built feedback control setup and discuss in Section 3 in greater detail the detachment stabilisation of the longest high-power W7-X discharge. In Section 4 the application of the impurity seeding feedback control for mitigation of baffle tiles heat loads is presented. Finally, in Section 5, we give an outlook for the hardware extension implemented for two upcoming experimental campaigns OP2.1 and OP2.2 with several ideas of application the feedback control of plasma detachment in W7-X.

2. System description and performance

The divertor gas injection was installed for the OP1.2 campaign at one upper and one lower divertor. Both systems featured a set of five fast piezo valves connected to capillary nozzle tubes arranged in the poloidal direction (see Fig. 2). The valve boxes were attached to the back side of the divertor which resulted in very short response times (<10 ms) of the gas flows on the control voltage. The design pressure range of 5 mbar up to 10 bar provided a large range of accessible atom/molecule flow rates of $10^{18} - 10^{23}$ s^{-1} of a variety of gasses (H_2, N_2, Ne, He, Ar, CH_4), their mixtures and isotopes. The piezo valves (Piezosystem Jena PX 500) were driven by power supplies (Piezosystem Jena 30V300) supplying voltage in the range of −20 V up to 130 V at a max. current of 300 mA. The analogue input signal (0–10 V) for the power supplies was provided by the feedback controller utilising a programmable microcontroller of type ATmega2560. The feedback controller software (written in c++) was based on the PID control type in which the output signal $u(t)$ for the actuator is calculated using the proportional, integral and derivative term of the error value $e(t)$ (deviation of the actual process value from its set point):

$$u(t) = K_p e(t) + K_i \int_0^t e(\tau) d\tau + K_d \frac{\mathrm{d}e(t)}{\mathrm{d}t}. \quad (1)$$

The parameters K_p, K_i and K_d need to be adapted according to the expected characteristics of the control process. These parameters as well as the controller cycle time (2–25 ms) and the gas pressure in the reservoir were validated and fine tuned in a lab test setup (see Fig. 1) using another microcontroller which simulated the expected diagnostic response as reaction to the gas valve actuation voltage. For example, for fine tuning of the electron density control parameters we modelled

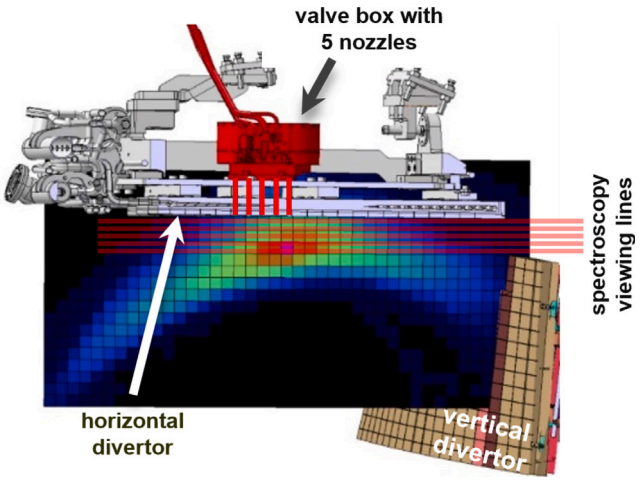

Fig. 2. CAD view of the gas injection system at the upper divertor.

the plasma density by considering the H_2 flow rate through the valve (with the delays caused by the valve reaction and gas flow through the nozzle), the fuelling efficiency and the effective particle confinement time in the plasma vessel. These values were known from similar experiments in the previous campaign OP1.2a. Linear relation of the gas flow rate with the valve actuation voltage was assumed. In the case of the plasma radiation control we assumed again a simple linear dependence of the radiation on the electron density and additionally anticipated for the expected delay of approx. 70 ms of the diagnostic response. These simulations revealed oscillations of the control parameter which were partially mitigated by optimisation of the differential component of the controller (see Fig. 3). In the real plasma discharges some further optimisation was needed and done, however with some remaining level of P_{rad} oscillations.

Several real-time diagnostic signals were connected to the controller as input values.

(a) The line integrated electron density ($\int n_e dl$) was provided by a single interferometer line-of-sight (LOS) going through the plasma centre. The applied PI controller with a cycle time of 2 ms featured very good precision of the controlled density of better than 1% (see Fig. 4).

(b) The total radiated power (P_{rad}) was extrapolated using a few LOS of two bolometer cameras which provided real-time values with a typical deviation of up to 10% from values generated using all channels taking the 3D geometry into account (see orange curve in Fig. 11). The P_{rad} signal arrived at the controller with typical delays of approx. 100 ms with respect to the valve actuation (see Section 4). This was partially by the intrinsic plasma impurity radiation reaction time and partially caused by electronic hardware processing time. Attempts to keep the control time significantly below 1 s (at typical controller cycle time of 10 ms) led to oscillations of P_{rad}. Including the differential component of the controller mitigated the oscillations to a level of +/−10% in the best case.

(c) Three out of 27 spectroscopy LOS viewing the divertor plasma (as indicated in Fig. 2) were connected to fast filterscopes with photomultipliers detecting emission lines of HeI, CII and CIII selected by appropriate interference filters. These spectroscopic signals from the divertor plasma allowed direct control of the plasma detachment from the divertor plates. For example, in experiment 20180920.032, CIII radiation intensity integrated along a horizontal LOS at a distance of approx. 6 cm to the divertor was very successfully controlled using H_2 fuelling. At the measurement location the CIII signal increased as the emission zone moved from the target towards the separatrix during transition into detachment. The plasma was stabilised over 6 s in partial detachment (the integral heat flux to all divertors reduced to approx. 30%, see Fig. 5; the total heat flux to all divertors was derived from

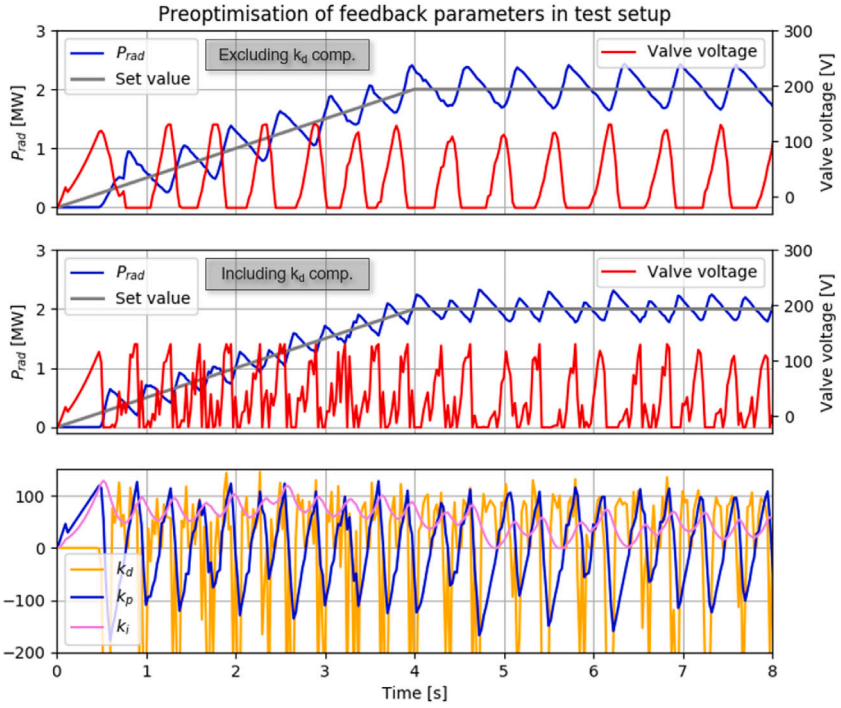

Fig. 3. Pre-optimisation of the feedback parameters for P_{rad} control. Top and middle panels: valve voltage and resulting P_{rad} curve without and with including the K_d component. Bottom panel: K_p, K_i and K_d contribution to the control signal in the case of including the K_d component.

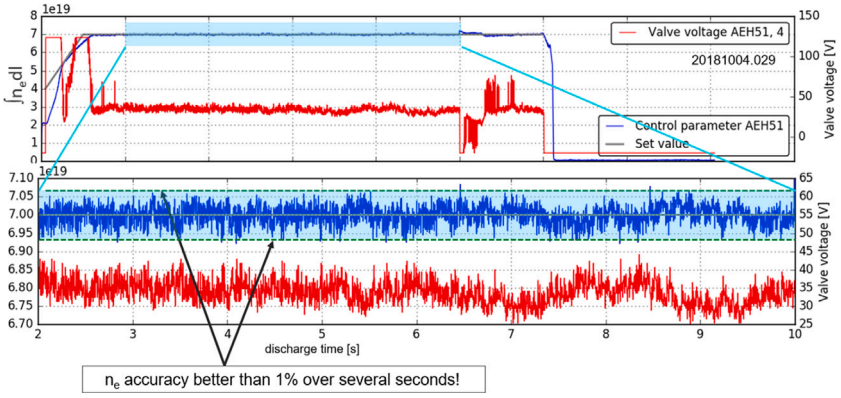

Fig. 4. $\int n_e dl$ provided by a core interferometer LOS was controlled with a precision of better than 1%.

IR images of all ten divertor modules [9]). Since the absolute level of CIII radiation in the divertor depends on the divertor plasma conditions using intensity ratios at different distances to the target seems more appropriate as detachment indicator and is described in Section 5.

(d) Radiation temperature of the electron cyclotron radiation (ECE) in the O2 mode was used as a proxy for the electron temperature (T_e) in the plasma core with the aim to reduce the gas flows and thereby to avoid plasma termination by radiation collapse in the case of too low absorption of the ECRH power in O2 mode. This signal was used as an additional boundary condition for the feedback controller which stopped the gas flows at T_e values falling below a preset threshold. In the discharge 20181016.012 four of the ECRH gyrotrons stopped operation in a sequence starting at 1.9 s of the discharge time (see Fig. 6). The T_e interlock sets in at approx. 2.5 s and interrupts the fuelling gas flow multiple times bringing effectively the feedback controller to keep the central T_e at a constant value of approx. 2 keV. The resulting electron density is falling in the course of the discharge as a reaction to the stepwise reduction of the available heating power.

The analogue values of all diagnostic signals were digitised and passed to the controller over a direct network fibre-optic cable connection. This proved to be very robust and showed no transmission failures throughout the entire campaign.

3. Detachment control in OP1.2b campaign

The longest (30 s) high-power discharge at W7-X (experiment 20181016.016) so far was kept in stable detachment over almost the entire discharge time using feedback control of interferometer density and H_2 fuelling through the divertor gas injection system. Two preparatory experiments were needed to develop the scenario. In the first step (experiment 20181010.027) the plasma density was ramped up slowly using the precise feedback control of $\int n_e dl$. Simultaneously, the behaviour of the total plasma radiation was sampled which typically showed a very strong increase of the radiation power in the onset of detachment, see Fig. 7. The high radiation level originates from intrinsic low-Z impurities (mainly carbon and oxygen) [4] and sets the maximum achievable plasma density for given heating power. We

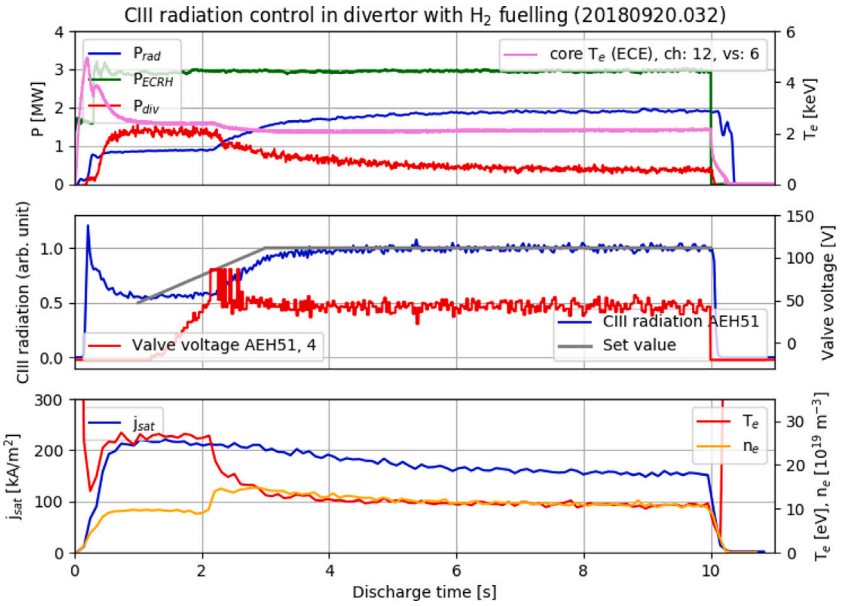

Fig. 5. Parameter time traces of a discharge feedback-controlled using CIII radiation in the divertor. Top: Heating and radiated power, integral heat flux to all divertors, electron temperature in the plasma core. Middle: Set and reached CIII emission in divertor, valve actuation voltage. Bottom: Ion saturation current, electron temperature and density measured with Langmuir probe #1 (closest position to strike line) in lower divertor 2 h in machine module 5.

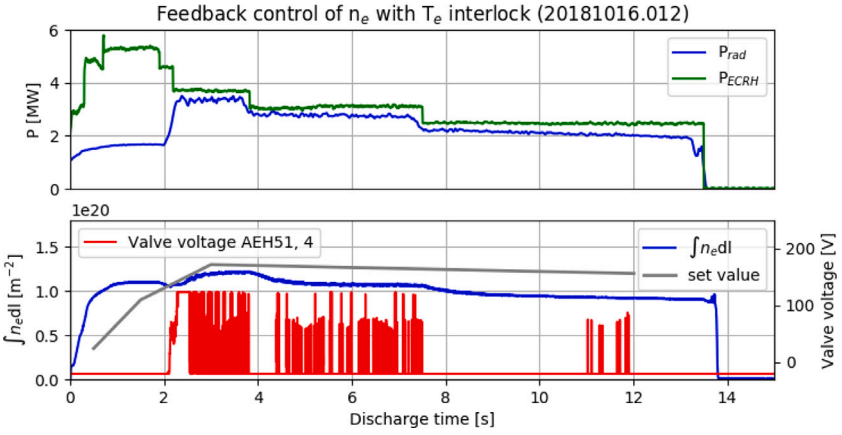

Fig. 6. Parameter time traces of a discharge with $\int n_e dl$ feedback control and active T_e interlock. Top: Heating and radiated power. Bottom: Set and reached value of $\int n_e dl$ as well as the gas valve actuation showing strongly reduced gas flows induced by the T_e interlock.

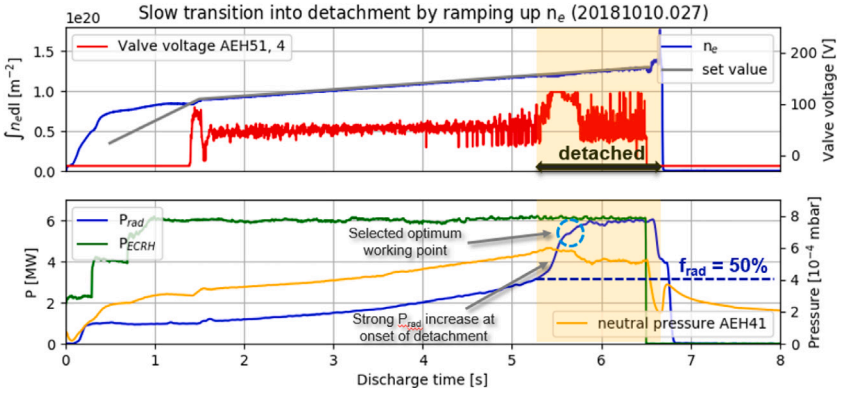

Fig. 7. Parameter time traces of a discharge in which the electron density was ramped up for a slow transition into detachment to sample the P_{rad} behaviour. Top: Set and reached value of $\int n_e dl$ as well as the gas valve actuation. Bottom: Neutral gas pressure in sub-divertor space, heating and radiated power with the choice of the optimum detachment working point with respect to radiation.

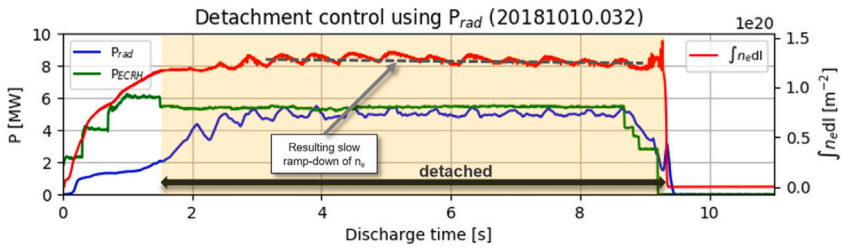

Fig. 8. Parameter time traces of a discharge with detachment control using P_{rad}. The dashed curve shows the decreasing trend of resulting $\int n_e dl$ needed to keep P_{rad} on a constant level.

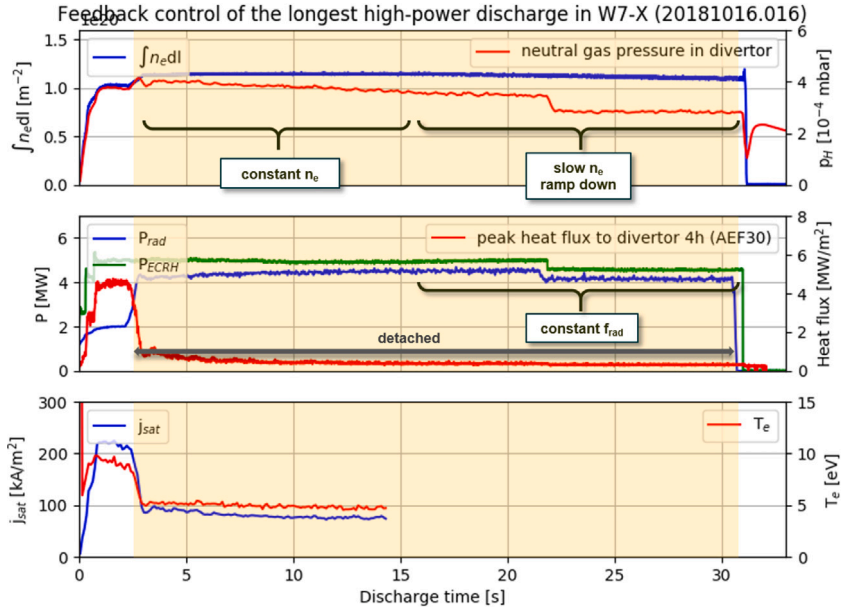

Fig. 9. Parameter time traces of the longest high-power W7-X discharge well stabilised in detachment using feedback control of $\int n_e dl$. Top: Reached value of $\int n_e dl$ with the phase of constant and of ramped-down values, average neutral gas pressure in the sub-divertor space of target modules 2 h in machine modules 30, 31 and 41. Middle: Heating and radiated power, peak heat flux to target module 4 h of the bottom divertor in machine module 3. Bottom: Ion saturation current and electron temperature measured with Langmuir probe #1 (closest position to strike line) in lower divertor 2 h in machine module 5 (note that the data is available only up to $t = 14.3$ s due to a failure of the data acquisition system).

selected an optimum working point in the detached plasma conditions with respect to radiation at the radiation fraction f_{rad} of approx. 80%–90%. In the second step this level of f_{rad} was feedback-controlled over 6 s of the experiment 20181010.032 using the total plasma radiation P_{rad} from the bolometer cameras, however, with the remaining oscillations (see Fig. 8). To avoid the oscillations, in the final experiment we turned back to the precise oscillation-free density control. The set point for the line integrated density was selected according to the levels (indicated with the dashed curve in Fig. 8) needed to keep a discharge with similar ECRH power in detached conditions with the desired radiation fraction: we kept $\int n_e dl$ at a constant level of 1.15×10^{20} m^{-2} in the first half (t < 16 s) of the discharge. The plasma was driven into detachment during the short density ramp at 2.5 s in which we observe characteristic changes of plasma and neutral gas parameters (as shown in Fig. 9): the neutral gas pressure reaches its maximum, the peak heat fluxes to the divertors reduce by factor 5 while the total radiated power reaches 80%–90% of the heating power, and the electron temperature and ion fluxes at the divertor reduce by factor 2. Even though in this discharge phase the electron density and heating power were kept constant, we observed slight increase of total radiated power which was likely due to continuous heating up of the uncooled first-wall components. This led to even more pronounced detachment (lower heat fluxes to divertor, lower T_e and j_{sat} at divertor plate), however accompanied by lowering of the neutral gas pressure. This roll-over of the neutral gas pressure at higher values of radiated power fraction is in-line with predictions with the EMC3-EIRENE code [1]. In the second half of the discharge (for t > 16 s) we applied a very slow ramp-down of $\int n_e dl$ to the value of 1.1×10^{20} m^{-2} in order to keep the radiated power fraction at a constant level which worked very well and allowed to keep the remaining 15 s of the discharge time in very well stabilised detachment. In future experiments physics-based scaling of P_{rad} as function of n_e, the heating power and Z_{eff} will be used for better control of total radiated power.

4. Mitigation of excessive heat loads to baffles

In the so called high-mirror magnetic configuration one vertical baffle tile (as shown in Fig. 10) experienced heat loads exceeding the specified value of 0.5 MW/m^2 in many cases. N_2 and Ne seeding was applied to increase the radiated power fraction which resulted in reduction of the heat loads to acceptable levels. In the experiment 20181009.041 at $t = 1$ s a 40 ms Ne pulse was applied which increased the radiated power by 0.5 MW (see Fig. 11). The signal increase was delayed by approx. 80 ms in this case. These typical delays caused oscillations when controlling the total plasma radiation provided by the bolometer cameras, for example as apparent later in the same discharge. From $t = 1.3$ s on until the end of the discharge N_2 seeding was applied and feedback-controlled using the total plasma radiation with targeted radiation fraction of approx. 55%. Some optimisation of the derivative term of the PID controller helped to reduce but not to completely avoid the oscillation. Despite the P_{rad} oscillation,

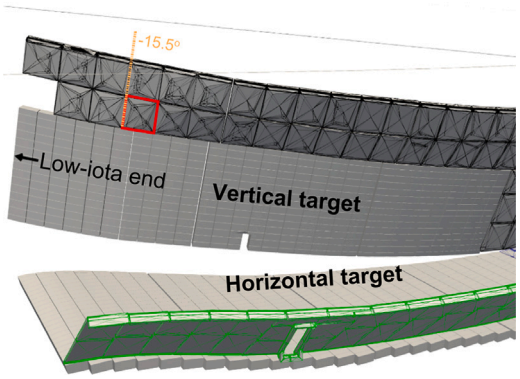

Fig. 10. CAD model showing in red the baffle tile typically overloaded with heat fluxes in the high-mirror magnetic configuration.

the seeding control scenario successfully reduced the heat load to the critical baffle to acceptable levels over the entire seeding time.

5. Upgrade and ideas for the next two campaigns

The very successful detachment stabilisation in W7-X by various feedback control schemes of the divertor gas fuelling and seeding encouraged us to strongly increase the capabilities of the system for the two upcoming experimental campaigns OP2.1 and OP2.2 (starting in fall of 2022 and 2023, respectively). The divertor gas injection system will be extended (keeping the same design) from two to all ten divertors. The set of real-time diagnostic input signals will be extended to provide additional control parameters in the plasma edge (neutral gas pressure in the divertor and in the midplane; divertor surface temperature) as well as to optimise the core plasma performance (diamagnetic plasma energy). Some of the signals will be only available for the campaign OP2.2. The controller hardware will be replaced by a real-time linux-based system extending the control capabilities beyond the PID controller type, e.g. to allow for maximisation, for including physics models and for machine-learning based algorithms.

Given the successful feedback control (in separate experiments) of plasma density with fuelling and of P_{rad} with nitrogen seeding (see also the description of the experiment 20181016.023 later in this section and shown in Fig. 13) it seems reasonable to combine these schemes in one experiment and apply two independent simultaneous PID controllers that use different gas injection systems with the aim to raise the plasma density and radiation to a certain level by fuelling and increase the radiation further by impurity seeding. In the case of too strong coupling between both controllers a single physics-based control algorithm for the two actuators (fuelling and seeding valve) will be applied to account for the dependencies to provide better prediction of the plasma reaction and by this more robust control. It is also planned to apply first simple machine-learning based algorithms to handle the increasing complexity of the W7-X control schemes resulting from the availability of more diagnostic signals for the detachment control. Looking at characteristic diagnostic signals in the plasma edge observed during the transition into detachment in the previous campaign some specific control schemes appear potentially interesting for the detachment stabilisation and optimisation and will also be tested during the next two experimental campaigns. In the experiment 20181010.030 detachment was stabilised with hydrogen fuelling feedback-controlled by the P_{rad} signal. Its oscillation led to variation of the electron temperature in the divertor plasma. The electron temperature and density in the plasma edge can be derived from intensity ratios of spectral lines of atomic helium [10–12]. Its small amounts can either reside in the plasma edge or be injected on purpose to even allow local measurements by the modulation of the gas flow in the beam. Fig. 12 (bottom) shows the T_e sensitive line ratio (706.5 nm/728.1 nm) of atomic helium (residing in small amount in the divertor plasma) measured along one LOS of the filterscope diagnostic (indicated in Fig. 2) 2.5 cm above the horizontal target plate. The clear reaction of the downstream T_e can be used to control detachment. Another option would be to localise and control the CII or CIII radiation front which moves towards the separatrix during transition into detachment [13], as a proxy for level of detachment. In experiment 20181016.023 CIII line emission was measured with three LOS of the filterscope diagnostic at three different distances (2, 6 and 8 cm) above the target. Line integrated electron density was feedback-controlled with H_2 fuelling and the plasma was simultaneously feed-forward seeded with N_2 to induce transition into detachment. In Fig. 13 line emission ratio ($I_{6cm}/(I_{2cm} + I_{8cm})$) is plotted which was used as a proxy for the emission front position. The maximum line ratio at approx. $t = 5.2$ s indicates the radiation front closest to the position of 6 cm above the target which corresponds to optimum detachment conditions (strongly reduced integral heat flux to all divertors, ion saturation current and T_e at the divertor plate as shown in Fig. 13). This indicates that the radiation front height above the target can be used to stabilise optimum detached conditions (by either impurity seeding or density increase by H_2 fuelling). Finally, one more interesting control scheme which will be tested is the detachment optimisation by maximisation of the neutral gas pressure in the sub-divertor space leading to maximum pumping rate of particles from the vacuum vessel. As shown in Fig. 7 (bottom) the neutral pressure in one of the divertors rolls over at too high radiation fraction due to strongly reduced ion fluxes to the target [1]. The feedback controller would stabilise the discharge at the working point of the maximum pressure.

6. Summary

The fuelling and impurity seeding control of two available W7-X divertor gas injection systems was equipped for the most recent campaign (OP1.2b) with feedback control capabilities using the interferometer electron density, the total plasma radiation from bolometer cameras and spectral line emission in the divertor plasma provided by filterscopes as input signals. Core electron temperature (from ECE diagnostic) was monitored and stopped the gas injection at too low T_e values which allowed to avoid radiative plasma collapses e.g. in the case of losing ECRH power during a discharge. PID control type was applied with pre-optimised control parameters in a lab test setup with a plasma signal simulator implemented using a programmable microcontroller. The feedback control system featured very high precision (better than 1%) of electron density control and allowed well stabilised detachment control based on the interferometer density and carbon emission in the divertor. The entire longest high-power discharge at W7-X so far was well stabilised in detachment using the density feedback control. The detachment was also stabilised using the total plasma radiation from bolometry, however in this case with remaining P_{rad} oscillation of approx. $+/-$ 10% due to delayed signals arriving at the controller. The system also proved useful to increase the plasma radiation to a level reducing heat loads to overloaded baffle tiles in the high-mirror magnetic configuration below the critical level of 1 MW/m^2. For the next two experimental campaigns, OP2.1 and OP2.2, the divertor injection system has been extended to all ten divertors. Additional diagnostic input signals (the neutral gas pressure, the target surface temperature and the diamagnetic plasma energy) for the controller are in preparation. Some detachment control ideas were presented based on the observations from the last campaign which will be tested in the upcoming campaigns. The controller hardware has been replaced by a real-time linux-based system opening a way to test in the next two campaigns more advanced control algorithms like maximisation, physic-based models, and machine-learning based approach.

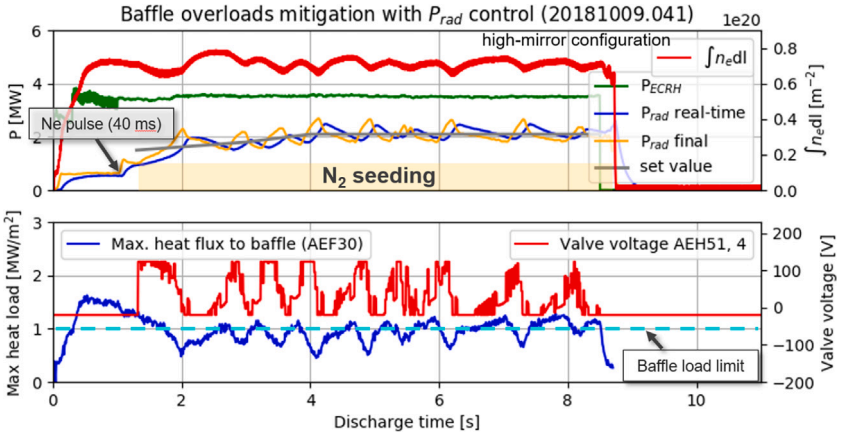

Fig. 11. Parameter time traces of a discharge with N_2 seeding using feedback control of total plasma radiation P_{rad}. Top: Heating power; real-time radiated power used for feedback control and post-processed radiated power generated from all channels taking the 3D geometry into account; resulting electron density. Bottom: Integral heat load to the critical baffle tile (shown in Fig. 10); valve actuation voltage.

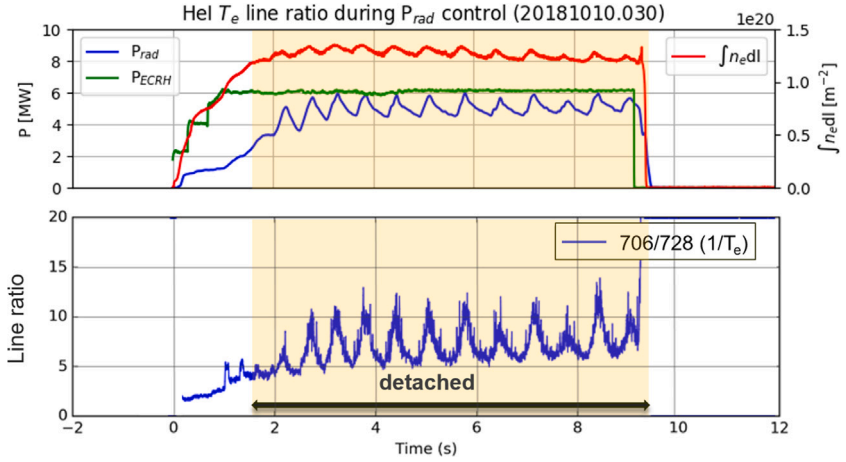

Fig. 12. Parameter time traces of a discharge with feedback control of total plasma radiation P_{rad}. Top: Heating and feedback-controlled radiated power; resulting electron density. Bottom: T_e dependent line ratio of atomic helium in the divertor plasma.

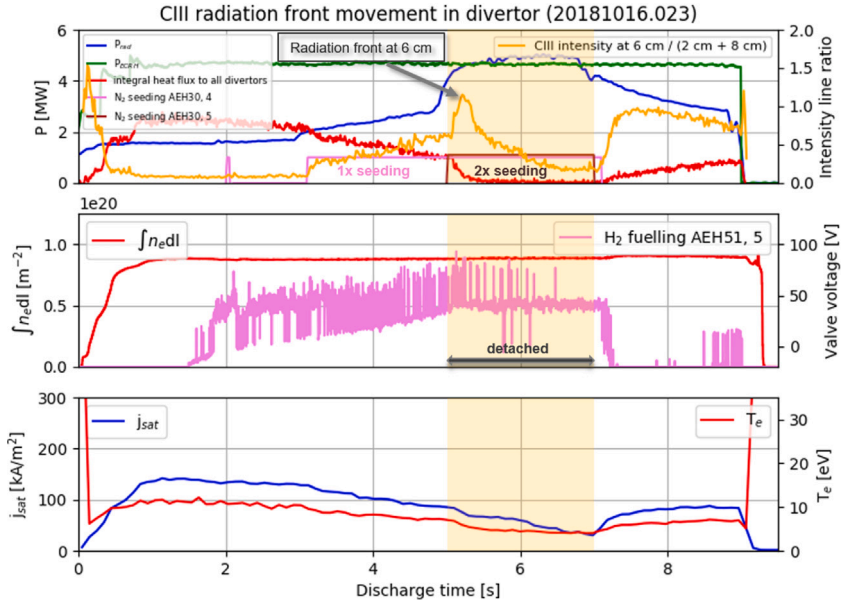

Fig. 13. Parameter time traces of a discharge with feed-forward N_2 seeding and feedback control of $\int n_e dl$ with H_2 fuelling. Top: Heating and radiated power, integral heat flux to all divertors, intensity ratio of CIII radiation indicating the radiation front position above the target. Middle: Line integrated electron density and fuelling gas actuation. Bottom: Ion saturation current and electron temperature measured with Langmuir probe #1 (closest position to strike line) in lower divertor 2 h in machine module 5.

CRediT authorship contribution statement

M. Krychowiak: Writing – original draft. **R. König:** Writing – review & editing. **T. Barbui:** Resources. **S. Brezinsek:** Resources. **J. Brunner:** Resources. **F. Effenberg:** Resources. **M. Endler:** Resources. **Y. Feng:** Resources. **E. Flom:** Writing – review & editing. **Y. Gao:** Resources. **D. Gradic:** Resources. **P. Hacker:** Resources. **J.H. Harris:** Resources. **M. Hirsch:** Resources. **U. Höfel:** Resources. **M. Jakubowski:** Resources. **P. Kornejew:** Resources. **M. Otte:** Resources. **A. Pandey:** Resources. **T.S. Pedersen:** Resources. **A. Puig:** Resources. **F. Reimold:** Writing – review & editing. **O. Schmitz:** Resources. **T. Schröder:** Software. **V. Winters:** Resources. **D. Zhang:** Resources. **W7-X team:** Resources.

Declaration of competing interest

The authors declare that they have no known competing financial interests or personal relationships that could have appeared to influence the work reported in this paper.

Data availability

Data will be made available on request.

Acknowledgements

This work has been carried out within the framework of the EUROfusion Consortium, funded by the European Union via the Euratom Research and Training Programme (Grant Agreement No 101052200 - EUROfusion). Views and opinions expressed are however those of the author(s) only and do not necessarily reflect those of the European Union or the European Commission. Neither the European Union nor the European Commission can be held responsible for them. This work was supported by the U.S. Department of Energy (DoE) under contract DE-SC0014210 and DE-AC02-09CH11466.

References

[1] Y. Feng, M. Jakubowski, R. König, M. Krychowiak, M. Otte, F. Reimold, D. Reiter, O. Schmitz, D. Zhang, C. Beidler, C. Biedermann, S. Bozhenkov, K. Brunner, A. Dinklage, P. Drewelow, F. Effenberg, M. Endler, G. Fuchert, Y. Gao, J. Geiger, K. Hammond, P. Helander, C. Killer, J. Knauer, T. Kremeyer, E. Pasch, L. Rudischhauser, G. Schlisio, T.S. Pedersen, U. Wenzel, V. Winters, the W7-X Team, Understanding detachment of the W7-X island divertor, Nucl. Fusion 61 (8) (2021) 086012, http://dx.doi.org/10.1088/1741-4326/ac0772.

[2] M. Jakubowski, M. Endler, Y. Feng, Y. Gao, C. Killer, R. König, M. Krychowiak, V. Perseo, F. Reimold, O. Schmitz, T. Pedersen, S. Brezinsek, A. Dinklage, P. Drewelow, H. Niemann, M. Otte, M. Gruca, K. Hammond, T. Kremeyer, M. Kubkowska, S. Jabłoński, A. Pandey, G. Wurden, D. Zhang, S. Bozhenkov, D. Böckenhoff, C. Dhard, J. Baldzuhn, D. Gradic, F. Effenberg, P. Kornejew, S. Lazerson, J. Lore, D. Naujoks, A.P. Sitjes, G. Schlisio, M. Ślęczka, U. Wenzel, V. Winters, the W7-X Team, Overview of the results from divertor experiments with attached and detached plasmas at Wendelstein 7-X and their implications for steady-state operation, Nucl. Fusion 61 (10) (2021) 106003, http://dx.doi.org/10.1088/1741-4326/ac1b68.

[3] F. Effenberg, S. Brezinsek, Y. Feng, R. König, M. Krychowiak, M. Jakubowski, H. Niemann, V. Perseo, O. Schmitz, D. Zhang, T. Barbui, C. Biedermann, R. Burhenn, B. Buttenschön, G. Kocsis, A. Pavone, F. Reimold, T. Szepesi, H. Frerichs, Y. Gao, U. Hergenhahn, S. Kwak, M. Otte, T.S. Pedersen, the W7-X Team, First demonstration of radiative power exhaust with impurity seeding in the island divertor at wendelstein 7-x, 59 (10), 2019, p. 106020, http://dx.doi.org/10.1088/1741-4326/ab32c4.

[4] D. Zhang, R. Burhenn, Y. Feng, R. König, B. Buttenschön, C. Beidler, P. Hacker, F. Reimold, H. Thomsen, R. Laube, T. Klinger, L. Giannone, F. Penzel, A. Pavone, M. Krychowiak, M. Beurskens, S. Bozhenkov, J. Brunner, F. Effenberg, G. Fuchert, Y. Gao, J. Geiger, M. Hirsch, U. Höfel, M. Jakubowski, J. Knauer, S. Kwak, H. Laqua, H. Niemann, M. Otte, T.S. Pedersen, E. Pasch, N. Pablant, K. Rahbarnia, J. Svensson, B. Blackwell, P. Drews, M. Endler, L. Rudischhauser, E. Wang, G. Weir, V. Winters, the W7-X Team, Plasma radiation behavior approaching high-radiation scenarios in w7-x, Nucl. Fusion 61 (12) (2021) 126002, http://dx.doi.org/10.1088/1741-4326/ac2b75.

[5] D. Eldon, H. Anand, J.-G. Bak, J. Barr, S.-H. Hahn, J.H. Jeong, H.-S. Kim, H.H. Lee, A.W. Leonard, B. Sammuli, G.W. Shin, H.Q. Wang, Enhancement of detachment control with simplified real-time modelling on the KSTAR tokamak, Plasma Phys. Control. Fusion 64 (7) (2022) 075002, http://dx.doi.org/10.1088/1361-6587/ac6ff9.

[6] J. Koenders, M. Wensing, T. Ravensbergen, O. Février, A. Perek, M. van Berkel, the.T.C.V. Team, the.EUROfusion.MST1. Team, Systematic extraction of a control-oriented model from perturbative experiments and SOLPS-ITER for emission front control in TCV, Nucl. Fusion 62 (6) (2022) 066025, http://dx.doi.org/10.1088/1741-4326/ac5b8c.

[7] T. Ravensbergen, M. van Berkel, A. Perek, C. Galperti, B.P. Duval, O. Février, R.J.R. van Kampen, F. Felici, J.T. Lammers, C. Theiler, J. Schoukens, B. Linehan, S. Komm, M. Henderson, D. Brida, M.R. de Baar, Real-time feedback control of the impurity emission front in tokamak divertor plasmas, Nature Commun. 12 (1) (2021) 1105, http://dx.doi.org/10.1038/s41467-021-21268-3.

[8] M. Bernert, F. Janky, B. Sieglin, A. Kallenbach, B. Lipschultz, F. Reimold, M. Wischmeier, M. Cavedon, P. David, M. Dunne, M. Griener, O. Kudlacek, R. McDermott, W. Treutterer, E. Wolfrum, D. Brida, O. Février, S. Henderson, M. Komm, X-point radiation its control and an ELM suppressed radiating regime at the ASDEX upgrade tokamak, Nucl. Fusion 61 (2) (2020) 024001, http://dx.doi.org/10.1088/1741-4326/abc936.

[9] M. Jakubowski, P. Drewelow, J. Fellinger, A. Puig Sitjes, G. Wurden, A. Ali, C. Biedermann, B. Cannas, D. Chauvin, M. Gamradt, H. Greve, Y. Gao, D. Hathiramani, R. König, A. Lorenz, V. Moncada, H. Niemann, T.T. Ngo, F. Pisano, T. Sunn Pedersen, Infrared imaging systems for wall protection in the w7-x stellarator (invited), Rev. Sci. Instrum. 89 (10) (2018) 10E116, http://dx.doi.org/10.1063/1.5038634.

[10] B. Schweer, G. Mank, A. Pospieszczyk, B. Brosda, B. Pohlmeyer, Electron temperature and electron density profiles measured with a thermal He-beam in the plasma boundary of TEXTOR, J. of Nucl. Mater. 196-198 (1992) 174–178.

[11] T. Barbui, M. Krychowiak, R. König, O. Schmitz, J.M. Muñoz Burgos, B. Schweer, A. Terra, Feasibility of line-ratio spectroscopy on helium and neon as edge diagnostic tool for wendelstein 7-x, Rev. Sci. Instrum. 87 (11) (2016) 11E554, http://dx.doi.org/10.1063/1.4962989, arXiv:https://aip.scitation.org/doi/pdf/10.1063/1.4962989 https://aip.scitation.org/doi/abs/10.1063/1.4962989.

[12] M. Griener, E. Wolfrum, M. Cavedon, R. Dux, V. Rohde, M. Sochor, J.M. Muñoz Burgos, O. Schmitz, U. Stroth, Helium line ratio spectroscopy for high spatiotemporal resolution plasma edge profile measurements at asdex upgrade (invited), Rev. Sci. Instrum. 89 (10) (2018) 10D102, http://dx.doi.org/10.1063/1.5034446.

[13] M. Krychowiak, R. König, F. Henke, T. Barbui, E. Flom, S. Kwak, J. Svensson, D. Gradic, Y. Feng, Y. Gao, M. Jakubowski, M. Otte, F. Reimold, O. Schmitz, V. Winters, D. Zhang, T.S. Pedersen, the W7-X Team, Gaussian process tomography of carbon radiation in the transition to detached plasmas in the Wendelstein 7-X stellarator, in: 47th EPS Conference on Plasma Physics, 2021, P1.1026.